Computational Study on the Existence of Organic Peroxy Radical-Water Complexes ($RO_2 \cdot H_2O$)

Jared Clark, Alecia M. English, and Jaron C. Hansen*

Department of Chemistry and Biochemistry, Brigham Young University, Provo, Utah 84602

Joseph S. Francisco

Department of Chemistry and Department of Earth and Atmospheric Sciences, Purdue University, West Lafayette, Indiana 47907

Received: September 10, 2007; In Final Form: November 8, 2007

The existence of a series of organic peroxy radical−water complexes [$CH_3O_2 \cdot H_2O$ (methyl peroxy); $CH_3CH_2O_2 \cdot H_2O$ (ethyl peroxy); $CH_3C(O)O_2 \cdot H_2O$ (acetyl peroxy); $CH_3C(O)CH_2O_2 \cdot H_2O$ (acetonyl peroxy); $CH_2(OH)O_2 \cdot H_2O$ (hydroxyl methyl peroxy); $CH_2(OH)CH_2O_2 \cdot H_2O$ (2-hydroxy ethyl peroxy); $CH_2(F)O_2 \cdot H_2O$ (fluoro methyl peroxy); $CH_2(F)CH_2O_2 \cdot H_2O$ (2-fluoro ethyl peroxy)] is evaluated using high level ab initio calculations. A wide range of binding energies is predicted for these complexes, in which the difference in binding energies can be explained by examination of the composition of the R group attached to the peroxy moiety. The general trend in binding energies has been determined to be as follows: fluorine ≈ alkyl < carbonyl < alcohol. The weakest bound complex, $CH_3O_2 \cdot H_2O$, is calculated to be bound by 2.3 kcal mol^{-1}, and the strongest, the $CH_2(OH)O_2 \cdot H_2O$ complex, is bound by 5.1 kcal mol^{-1}. The binding energy of the peroxy radical−water complexes which contain carbonyl and alcohol groups indicates that these complexes may perturb the kinetics and product branching ratios of reactions involving these complexes.

I. Introduction

Organic peroxy radicals (RO_2) are products of the atmospheric oxidation of hydrocarbons, and they represent an important class of intermediates[1,2] leading to the formation of tropospheric ozone, as well as playing a role in managing the HO_x (OH and HO_2) radical budget. Organic peroxy radicals are formed from the reaction of hydrocarbons with OH, Cl, or NO_3 radicals, followed by the subsequent addition of O_2 to the hydrocarbon radical.[3,4]

$$RH + OH, Cl \text{ or } NO_3 \rightarrow R\bullet + H_2O, HCl \text{ or } HNO_3 \quad (1)$$

$$R\bullet + O_2 + M \rightarrow RO_2 + M \quad (2)$$

One mechanism for the production of tropospheric ozone as well as the major loss process for peroxy radicals under polluted conditions is the reaction of RO_2 radicals with NO.

$$RO_2 + NO \rightarrow RO + NO_2 \quad (3)$$

$$NO_2 + h\upsilon \rightarrow NO + O \quad (4)$$

$$O + O_2 \rightarrow O_3 \quad (5)$$

A second association/isomerization product path to produce alkyl nitrates has been observed. The mechanism is postulated to be[5]

$$RO_2 + NO \rightarrow ROONO^* \quad (6)$$

$$ROONO^* + M \rightarrow RONO_2 \quad (7)$$

The product branching ratio (k_3/k_7) has been shown to depend on the size of the RO_2 radical as well as exhibit both a pressure and negative temperature dependence.[6]

Recent work by Butkovskaya et al.[7] probing the effects of temperature and water vapor on the $HO_2 + NO$ reaction kinetics and product branching ratio has shown that the yield of HNO_3 (the association/isomerization) product increases by 90% in the presence of modest amounts of water vapor. The increased HNO_3 production as a function of increasing water vapor was explained as occurring because of the formation of a $HO_2 \cdot H_2O$ complex during the reaction mechanism.

Under conditions indicative of the upper troposphere, the formation of HNO_3 from the $HO_2 + NO$ reaction in the presence of water vapor would contribute 23% to the total loss process of HO_x radicals. This study highlights the necessity of understanding the rates and products of peroxy radical reactions under atmospheric conditions where peroxy−water complexes may exist

The simplest RO_2 radical is the HO_2 radical. Experimental measurements on the kinetics of the HO_2 self-reaction indicate a water vapor dependence to the reaction rate coefficient. The water vapor enhancement is shown to increase with decreasing temperatures, which has been explained by the formation of a $HO_2 \cdot H_2O$ complex which is speculated to form during the reaction mechanism. Recently, the existence of this peroxy−water complex has been confirmed by Suma et al.,[8] who were able to observe pure rotational transitions for the complex in a supersonic jet by means of a Fourier transform microwave spectrometer. Kanno et al.,[9] using frequency modulated diode laser spectroscopy, have successfully measured the equilibrium

* To whom correspondence should be addressed. E-mail: jhansen@chem.byu.edu. Fax: (801) 422-0153. Telephone: (801) 422-4066.

10.1021/jp077266d CCC: $40.75
Published on Web 01/29/2008

constant of the $HO_2 \cdot H_2O$ complex. These experimental results are complemented by ab initio computational studies[10] that have reported the lowest energy conformer vibrational frequencies and binding energies for the $HO_2 \cdot H_2O$ and $HO_2 \cdot (H_2O)_n$ complexes.

Recent results suggest that upward of 30% of HO_2 radicals in the atmosphere are complexed with water under typical atmospheric conditions.[9,10] Modeling studies indicate that the water vapor enhancement cannot be ignored when modeling atmospheric processes.[11] We propose that RO_2 radicals in the presence of water may form similar $RO_2 \cdot H_2O$ complexes. The existence of $RO_2 \cdot H_2O$ would serve to perturb the reactivity of RO_2 radicals and consequently affect their kinetics and product branching ratios. This has not yet been considered in models incorporating RO_2 radicals.

Recently, organic films and reverse micelle formation have been proposed as one mechanism for atmospheric aerosol production.[12−15] These mechanisms suggest that water is encapsulated by organic molecules with hydrophilic heads directed inward and hydrophobic ends directed outward. Processing of these ultra-fine aerosols is initiated by reactions with atmospheric radicals that transform the surface of these aerosols into hydrophilic surfaces which can grow by water accretion and form cloud condensation nuclei. The formation of the peroxy radical-water complexes investigated in this study may represent the first stages of this proposed mechanism for the process of aerosol formation under atmospheric conditions.

The work presented here is the first study involving six of the most prominent atmospherically relevant RO_2 radicals and their water complexes. The important question raised by this work is whether organic peroxy radical water complexes exist. This work will illustrate the possible influence that $RO_2 \cdot H_2O$ complexes may have on the spectroscopy, kinetics and measurement of RO_2 radicals.

II. Methods

The Gaussian 98, revision A.11.3[16] suite of programs was used to carry out ab initio calculations for H_2O and each of the RO_2 and $RO_2 \cdot H_2O$ complexes under consideration in this paper. Electron correlation was included and evaluated using unrestricted second-order Møller-Plesset perturbation theory (MP2),[17] quadratic configuration interaction with single, double, and triple excitations, QCISD(T),[18,19] coupled cluster with single, double, and perturbative triple excitations, CCSD(T),[20,21] and Brueckner doubles, BD(T).[22,23] Initial geometry and optimization work was performed using density functional methods (DFT), involving Hartree−Fock (HF)[24−26] and Becke three parameter exchange functional with the Lee, Yang, and Parr correlation functional (B3LYP).[27−30]

Basis sets used for the currently considered computations are of the general types, 6-31G and 6-311G.[31−35] Initial search optimizations and computations, including frequency calculations, used the 6-31G with the addition of diffuse functions on second-row atoms, as well as d- and p- polarization functions being added to the second-row atoms and the hydrogen atom, respectively. All other calculations involved the 6-311G basis set with added diffuse functions to both the hydrogen and second-row atoms, in addition to various combinations of polarization functions [6-311++G(d,p), 6-311++G(2d,2p), and 6-311++G(2df,2p)].

Interaction energies for the complexes were computed by taking the difference between the complex and isolated monomer sum. Zero-point vibrational energy[36,37] corrections computed at the B3LYP/6-31+G(d,p) level were applied to each interaction energy. The counterpoise (CP) procedure[38,39] was used at the MP2(full)/6-311++G(2d,2p) level to correct the interaction energy for basis set superposition error (BSSE).[40] Charges on individual atoms were calculated via the natural population method.[41]

The lowest energy peroxy radical conformation for each complex was found through a systematic evaluation of the potential energy surface defined by rotations of all bonds within each radical that, when rotated, would define a different molecular conformation. For each considered, bond rotations increments of 30° were used. These initial geometry calculations were performed at the HF/6-31G(d,p) level, followed by a frequency calculation to verify the absence of imaginary frequencies, and finished with an MP2(full)/6-31G(d,p) single-point calculation. Once a group of lowest energy structures was identified, optimizations using B3LYP and MP2(full) levels of theory with 6-311++G(d,p) and 3−11++G(2d,2p) basis sets were performed to identify the lowest energy structure. Identification and optimization of the lowest energy complex for each peroxy radical species was performed using proprietary software developed on site.[42] This software arrived at each lowest energy $RO_2 \cdot H_2O$ complex by first optimizing each of the lowest energy RO_2 molecules in the presence of a randomly oriented water molecule, placed within a sphere surrounding the radical with a volume, in part, defined by the size of the radical species. Constraints were placed on each randomly generated complex as to ignore nonsensical geometries, such as those that might arise having two hydrogen atoms occupying the same space. Five hundred initial geometries were optimized for each peroxy radical as per the procedure for the monomer species and a lowest energy structure was identified. All of the lowest energy structures were further evaluated at the QCISD(T), CCSD(T), and BD(T) levels of theory via single-point calculations, each with the 6-311++G(2d,2p) set of basis functions.

Calculations defining the contribution of the C−H···O hydrogen bonds to complex stabilization were performed by generating a series of $RO_2 \cdot H_2O$ geometries that incrementally removed the interacting water oxygen from the vicinity of the contributing C−H proton donating groups. Optimizations carried out were at the HF/6-311++G(d,p) level followed by an MP2(full)/6-311++G(2d,2p) single point calculation.

III. Results

The stabilization of atmospheric complexes comprising peroxy radical and water moieties is anticipated to arise primarily from traditional A−H···B hydrogen bonding (where A and B are highly electronegative atoms) and van der Waals interactions. The primary hydrogen bond formed in the molecular complexes, within the context of the present work, see Figure 1, has water acting as the hydrogen donor and an oxygen in the peroxy radical acting as the hydrogen acceptor through either the peroxy functionality itself (see Figure 1, panels A and B and E−H) or through other oxygen containing functionalities present in the radical, such as a carbonyl group (see Figure 1C,D). Each of the geometries in Figure 1 also seem to indicate additional molecular stabilization via significant, albeit weaker C−H···O_w hydrogen bonding interactions, with the water oxygen acting as the hydrogen acceptor and a C−H group acting as the hydrogen donor. The nomenclature of such an interaction is still in general debate, but recent work by Scheiner[43] et al. as well as that by Popelier[44] et al. has indicated that such a distinction is appropriate. For the sake of discussion here, reference to C−H···O interactions will be referred to as CHO

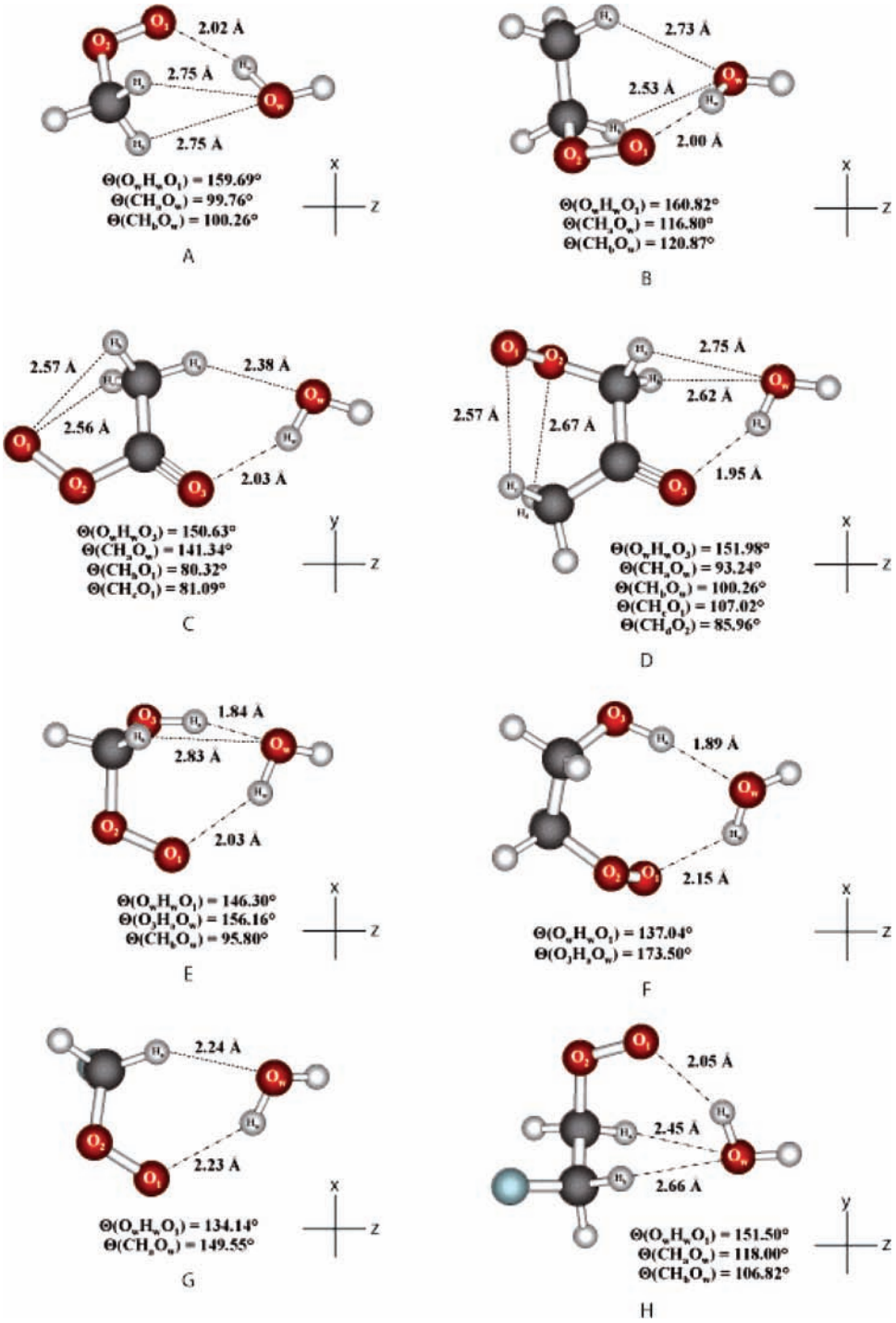

Figure 1. Optimized structures are at the MP2(full)/6-311++G(2df,2p) level. Bond lengths are reported in angstroms. A = $CH_3O_2 \cdot H_2O$; B = $CH_3CH_2O_2 \cdot H_2O$; C = $CH_3C(O)O_2 \cdot H_2O$; D = $CH_3C(O)CH_2O_2 \cdot H_2O$; E = $CH_2(OH)O_2 \cdot H_2O$; F = $CH_2(OH)CH_2O_2 \cdot H_2O$; G = $FCH_2O_2 \cdot H_2O$; H = $FCH_2CH_2O_2 \cdot H_2O$.

bonds. The importance of CHO bond interactions is not limited to small molecular complexes, like those of interest here, but has been recognized as an essential part to the geometric determination of larger systems that include but are not limited to nucleic acids,[45−48] proteins,[49−52] and carbohydrates.[53,54] The role of CHO_w hydrogen bonds in the coordination of water molecules has been demonstrated through an extensive review of neutron diffraction data extracted from the Cambridge Database[55] that provide hydrogen positions that have been experimentally determined to ±0.01 Å and better.[54] This later information demonstrates that any CHO_w bonds present in the peroxy radical/water complexes cannot be neglected in any description of the factors leading to complex stabilization.

Calibration. In addition to the eight peroxy radical/water complexes investigated herein, two calibration systems were also studied as a means to validate the methodologies used and to place the results presented in this work into a workable context. These two systems, hydroperoxy/water ($HO_2 \cdot H_2O$) and hydroperoxy/methanol ($HO_2 \cdot CH_3OH$) have been examined via computational and experimental means[10,56,57] and therefore present a reasonable basis for calibration. Table 1 contains the calculated binding energies for the two complexes compared to previously published results.

For the $HO_2 \cdot H_2O$ system, the minimum energy structure binding energy was calculated at the CCSD(T)/6-311++G(2df,-2p)//MP2(full)/6-311++G(2df,2p) level, to be 9.3 or 7.2 kcal

TABLE 1: Relative Binding Energies (kcal mol^{-1}) for the $HO_2 \cdot H_2O$ and $HO_2 \cdot CH_3OH$ Complexes

	$HO_2 \cdot H_2O$ binding energy	
levels of theory	D_e	D_0
MP2(full)/6-311++G(2df,2p)	9.6	7.5
QCISD(T)/6-311++G(2df,2p)//MP2(full)/6-311++G(2df,2p)	9.3	7.2
CCSD(T)/6-311++G(2df,2p)//MP2(full)/6-311++G(2df,2p)	9.3	7.2
BD(T)/6-311++G(2df/2p)//MP2(full)/6-311++G(2df,2p)	9.3	7.2
CCSD(T)/6-311++G(2df,2p)//B3LYP/6-311++G(2df,2p)[10]	9.4	6.9
experiment[55]	8.6 ± 3.8	
	$HO_2 \cdot CH_3OH$ binding energy	
levels of theory	D_e	D_0
MP2(full)/6-311++G(2df,2p)	10.6	8.8
QCISD(T)/6-311++G(2df,2p)//MP2(full)/6-311++G(2df,2p)	10.2	8.4
CCSD(T)/6-311++G(2df,2p)//MP2(full)/6-311++G(2df,2p)	10.2	8.4
BD(T)/6-311++G(2df/2p)//MP2(full)/6-311++G(2df,2p)	10.2	8.4
CCSD(T)/6-311++G(3df,3pd)//MP2(full)/6-311++G(3df,3pd)[54]	10.5	8.5
experiment[54]	8.9 ± 1.1	

mol^{-1} when corrected for the vibrational zero point energy. Aloisio et al.[10] reported a zero-point binding energy for the same hydroperoxy-water complex of 6.9 kcal mol^{-1}, optimized at the CCSD(T)/6-311++G(2df,2p)//B3LYP/6-311++G(2df,2p) level. In another paper, Aloisio et al.[57] report an experimentally determined value of 8.6 ± 3.8 kcal mol^{-1}. Although this experimental value deviates by more than 1.4 kcal mol^{-1} from the calculated value, our reported value falls within the reported experimental error.

Christensen et al.[56] have reported both calculated and experimental values for the binding energy of the $CH_3OH \cdot HO_2$ system. In their determination, the CCSD(T)/6-311++G(3df,-3pd)//MP2/6-311++G(3df,3pd) calculation of the binding energy gave an energy of 10.5 kcal mol^{-1} and a vibrational zero-point corrected energy of 8.5 kcal mol^{-1}, which are both in very good agreement with our values, calculated at the CCSD-(T)/6-311++G(2df,2p)//MP2(full)/6-311++G(2df,2p), of 10.2 and 8.4 kcal mol^{-1}, respectively. The reported experimental value of 8.9 ± 1.1 kcal mol^{-1} is again in excellent agreement with our numbers.

Geometry. A review of the optimized structures in Figure 1 reveals two significant structural similarities, regardless of functionalization. The first is the tendency for the RO_2 radical and water molecules to form 6 to 8 member cyclic structures upon complexation. In reference to this cyclization, there is clearly a preference for six member structures with nearly two-thirds of the perceived ring assemblies having this organization. Both seven- and eight-member ring geometries also exist, but within the scope of the structures covered in this work, they are only present in geometries that also contain a six membered group. One rationalization for the observed cyclic organization of these complexes arises from the ability of the water molecule to simultaneously act as a proton donor and acceptor. Examination of Figure 1 shows that each water molecule invests in an $O_w-H\cdots O_c$ type hydrogen bond with various acceptor functionalities within the monomer. With the exception of structures C and D, where the acceptor moiety is a carbonyl oxygen, the involved acceptor atom is the terminal oxygen of the $-O_2$ (peroxy) functionality. If this interaction constituted the sole point of interaction between the two monomers, the coordination potential of the water would be left unsatisfied, resulting in an "available" acceptor potential.[54] In the event that no other group is present in the relevant locality, such a potential would, of necessary, remain unfulfilled. Typically, however, there are eligible groups on hand that are able to coordinate with water and fulfill this potential. Commonly, such groups include NH, OH, and M^+. The structures herein presented also demonstrate the ability of CH groups (second structural similarity) to coordinate with water in the same way as NH and OH groups (Figure 1)[54] do, although this phenomenon is by no means germane to the present context.

In their review of neutron diffraction data, Steiner and Saenger[54] point out that a water molecule most frequently accepts two hydrogen bonds, preferably one from XH (X = O or N) and one from CH. The resulting coordinated geometry, although variable, is often tetrahedral. Steiner and Saenger conclude that one of the main functions of CH donors is the completion of tetrahedral coordination geometries when stronger donating species are not present. The most strongly bound complex (E), unlike the other seven structures in Figure 1, contains both OH and CH donor groups and manifests a distorted tetrahedral configuration. Complex F shares the strong OH donor group of E, but lacks a second coordinating CH species, which may explain the lower relative stability of this complex in relation to E. The remaining complexes are either 1 or 2 proton donating complexes, solely through CH functionalities. Complexes A and B both possess two CH proton contributing groups and each has a similarly distorted tetrahedral coordination geometry, which is reflected in their nearly identical binding energies. Complexes C and D both have CH groups that contribute to water coordination, but they also have CH groups involved in the coordination of the $-RO_2$ group. The interactions most likely in play are demonstrated in Figure 1C,D. The distribution of CH groups involved in CH complexation in C and D is 1:2, which is also reflected in the relative binding energies of the two complexes, although the manner of $-RO_2$ complexation most likely plays in the difference between the two. A similar 1:2 situation is evident in structures G and H. Complex H has two coordinating CH groups, similar to structure B, but demonstrates greater complex stability. In all likelihood, the dissimilarity arises from the augmented proton donating capacity of the CH groups as a result of the F atom being present. Structure G, distinguished as the least stable compound of the group, has but one CH coordinating group.

The nature of hydrogen bonds, in general, tends toward a linear geometry[43,58,59] and deviation from linearity frequently translates into a weakening of the interaction.[43] It has also been demonstrated that CHO bonds are less susceptible to weakening than their $O-H\cdots O$ counterparts[60,61] when bent. In the case of water, the weakening of the interaction energy for $O-H\cdots O$ interaction is on the order of 1−1.5 kcal mol^{-1} for a range of 120−240°.[43] Outside this range, the energy can change by as much as 3 kcal mol^{-1}. In contrast, the CHO interaction energy changes by ∼0.2−1 kcal mol^{-1} over this same range, making

TABLE 2: Relative Binding Energies for All Complexes. Relative Energies Are Reported in kcal mol^{-1}

	D_E[a]				D_O[a]				$D_{O,CP}$[a]			
	MP2	QCISD(T)	CCSD(T)	BD(T)	MP2	QCISD(T)	CCSD(T)	BD(T)	MP2	QCISD(T)	CCSD(T)	BD(T)
$CH_3O_2 \cdot H_2O$	5.3	5.1	5.1	5.1	4.4	4.1	4.1	4.1	2.6	2.3	2.3	2.4
$CH_3CH_2O_2 \cdot H_2O$	5.8	5.5	5.5	5.5	4.6	4.3	4.3	4.3	2.8	2.5	2.5	2.5
$CH_3C(O)O_2 \cdot H_2O$	5.6	5.5	5.5	5.5	4.5	4.5	4.5	4.5	2.9	2.9	2.9	2.9
$CH_3C(O)CH_2O_2 \cdot H_2O$	7.0	6.9	6.9	6.9	5.9	5.8	5.8	5.8	4.0	4.0	4.0	4.0
$CH_2(OH)O_2 \cdot H_2O$	9.8	9.4	9.4	9.4	7.9	7.5	7.5	7.5	5.5	5.1	5.1	5.1
$CH_2(OH)CH_2O_2 \cdot H_2O$	8.3	7.7	7.7	7.7	6.4	5.9	5.9	5.9	4.3	3.8	3.7	3.7
$FCH_2O_2 \cdot H_2O$	4.5	4.6	4.6	4.6	3.5	3.6	3.6	3.6	2.1	2.1	2.1	2.1
$FCH_2CH_2O_2 \cdot H_2O$	7.0	6.9	6.9	6.9	5.6	5.5	5.5	5.5	−3.7	3.5	3.5	3.5

it a faithful coordinating partner if present. The variation in the range depends in a large part upon the nature of any functional groups that may be acting upon the CH moiety. This sensitivity to geometry is demonstrated again in the eight complexes shown in Figure 1. Analyzed collectively, the O−H···O and C−H···O interactions show a definite statistical correlation between the bond angle of the interacting triad and the associated H···O bond length, which itself is a reflection of the magnitude of the stated interaction. Additionally, within each complex O−H···O interactions are seen to depart less from the optimum (180°) than C−H···O do, consistent with the developed paradigm. This relationship is helpful in describing the relative stabilities of hydrogen-bonded complexes. For example, structures A and B have roughly identical binding energies, with that of B being only slightly higher. This deviation, however, is not wholly unexpected. Both complexes have a similar number and type of hydrogen bonds. Each has a O_w−H···O bond angle of 159.69° and 160.82°, respectively. The difference in the two geometries is the bond angles of the two C−H···O interactions. In complex A, the two C−H···O bonds make angles of 99.76° and 100.26°, whereas in structure B, the angles are 116.80° and 120.87°. The later angles are more linear and are expected to attribute to a more stable binding interaction, as they are observed to do. With the exception of complex G, each $RO_2 \cdot H_2O$ species can be described in this manner. On examination, it can be seen that the most linear interaction within this complex is the CHO bond, with an angle of 149.55°, as compared to the 134.14° O−H···O bond. The stronger proton donating ability of the FC−H···O likely plays a role in this phenomenon. The overall result is a destabilization of the complex relative to A.

Binding Energy. The CCSD(T)/6-311++G(2d,2p) zero-point adjusted binding energies corrected for BSSE for the $CH_3O_2 \cdot H_2O$ and $CH_3CH_2O_2 \cdot H_2O$ complexes are found to be 2.3 and 2.5 kcal mol^{-1}, respectively. The binding energy increases with the addition of a carbonyl moiety in the R group of the peroxy radical. The corresponding corrected binding energies for the $CH_3C(O)O_2 \cdot H_2O$ and $CH_3C(O)CH_2O_2 \cdot H_2O$ complexes are calculated to be 2.9 and 4.0 kcal mol^{-1}, respectively. Further strengthening of the binding energy is observed for complexes that include an −OH moiety in the R group of the peroxy radical. The CCSD(T) level corrected binding energies are found to be 5.1 and 3.7 kcal mol^{-1} for the $CH_2(OH)O_2 \cdot H_2O$ and $CH_2(OH)CH_2 \cdot H_2O$ complexes, respectively. Finally, the corrected binding energies for the $FCH_2O_2 \cdot H_2O$ and $FCH_2CH_2O_2 \cdot H_2O$ complexes were computed to be 2.1 and 3.5 kcal mol^{-1}, respectively.

Analysis of results from Table 2 shows the following trend of stabilization based on the attached functional groups to the peroxy radical: fluorine ≈ alkyl < carbonyl < alcohol.

Electron Density Shifts. A useful method for describing how the electron density of the peroxy-radical and water molecules shifts throughout the entire space occupied by the newly formed complexes is through electron density difference maps. Maps for the eight complexes of topic are provided in Figure 2, with a contour of 0.0007 e/au^{3}computed at the MP2(full)/6-311++G-(2d,2p) level. Areas of electron gain are represented by light (yellow) regions and those of electron loss, dark (black) regions. Generally, O−H···O hydrogen bonds and CHO interactions are evidenced by a region of electron density loss around the proton acceptor atom.[43] Moving along the axis of the hydrogen bond toward the bridging hydrogen atom, a region of electron density gain is then observed followed by another region of electron density loss around the bridging proton. In the context of the work presented here, each hydrogen bond interaction within the eight complexes in Figure 1 can be demonstrated to exhibit this electron density shift pattern. In addition, these maps describe no fundamental difference in the two types of hydrogen bonding interactions.

Vibrational Spectra. Changes in the vibrational spectra of each radical species may also provide evidence for the existence of these weaker C−H···O stabilizing interactions. In the case of conventional hydrogen bonds, changes in the vibrational spectra, upon complexation, typically demonstrate a red-shift in the frequency associated with the O−H stretch and experience an enhancement in intensity.[43] In contrast, experimental observations seem to indicate that the reverse pattern is generally true for stabilizing interactions involving the CH group;[62−65] that is, they show a blue-shift in the frequency associated with the C−H stretch and experience a reduction in intensity. Such trends can be useful in the formulation of models describing hydrogen bond and CHO bond behavior, but it should be remembered that, in practice, the assignment of a particular stretching frequency to a single molecular OH or CH vibration is not always straight forward. In the case of CHO interactions, it is often the case that multiple hydrogens are bonded to the carbon atom of the CHO triad and that the stretching vibrations of these additional hydrogens are described by the same stretching frequency as the CH stretch of interest. It follows that the sum vibrational frequency describing the various CH vibrations will be a result of not only the CHO interaction but any additional interactions the other hydrogens may be involved in. Consequently, a CHO interaction may be found to deviate from the general model of behavior expected of such interactions. Table 3 lists the changes in the asymmetric stretching frequencies and intensities related to the O−H (shown in bold) and C−H stretches in each of the complexes pictured in Figure 1. Each of the OH stretching frequencies, as expected, is shifted toward the red and shows a marked increase in intensity. Faithful adherence to the characteristics of CH stretching frequency and intensity behavior upon formation of CHO bond interactions is demonstrated for the majority of the complexes of interest here. The observed range of CH blue-shifted frequencies (1.10−24.01 cm^{-1}) is consistent with those observed by Yanliang et al.[43] in their ab initio computational study of F_nCH−X complexes (n = 1, 2, or 3; X = H_2O, CH_3OH, H_2CO; angle CHX constrained to be 180°), where blue-shifted frequency values of 7−47 cm^{-1}

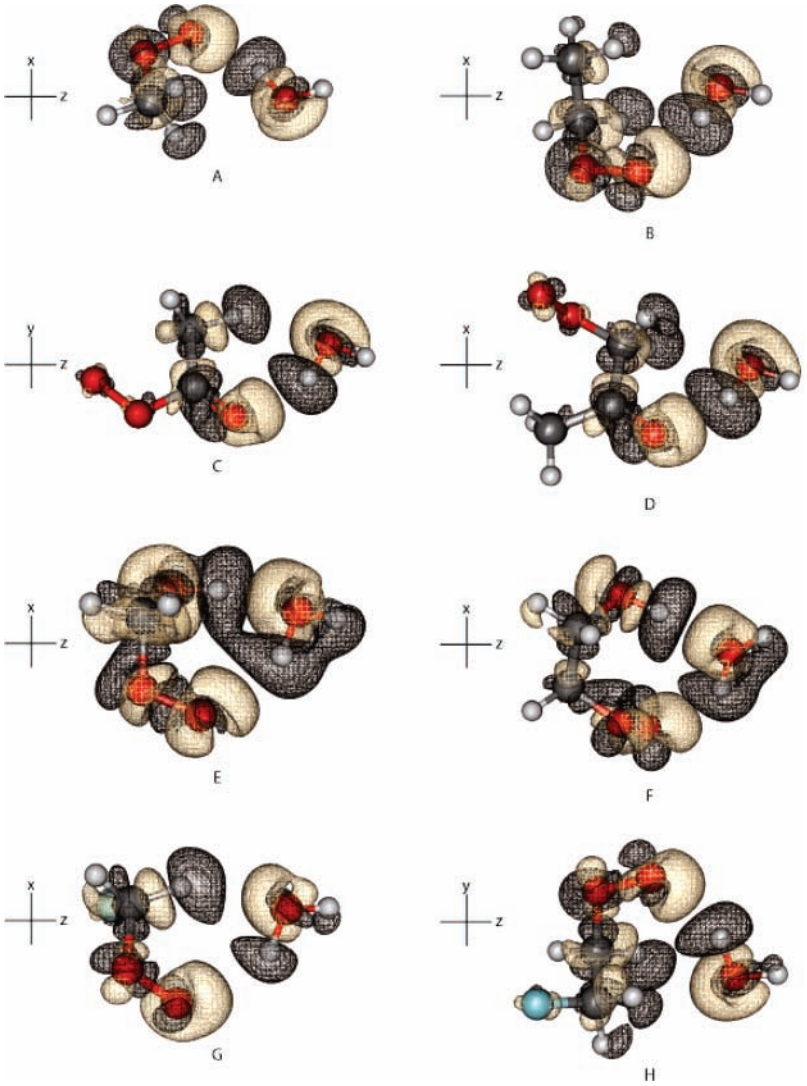

Figure 2. Electron density difference maps for the optimized structures. Dark and light regions represent electron density loss and gain, respectively, upon complex formation, relative to the isolated subunits. The contour shown is 0.0007 e/au,^{3} calculated at the MP2/6-311++G(2d,2p) level.

TABLE 3: Changes in the Frequency and Intensity Ratio of the Asymmetric CH Stretch and the OH Stretch (where Applicable) in the Peroxy Radical Subunit

complex	$\Delta\nu$, cm^{-1}[a]	I/I_o[b]
$CH_3O_2{\cdot}H_2O$	7.91	0.56
	10.09	0.42
$CH_3CH_2O_2{\cdot}H_2O$	10.28	0.43
	10.02	0.48
$CH_3C(O)O_2{\cdot}H_2O$	−1.67	5.48
$CH_3C(O)CH_2O_2{\cdot}H_2O$	1.72	20.70
$CH_2(OH)O_2{\cdot}H_2O$	1.10	0.97
	−272.29	**8.99**
$CH_2(OH)CH_2O_2{\cdot}H_2O$	**−172.32**	**7.52**
$FCH_2O_2{\cdot}H_2O$	7.79	0.45
$FCH_2CH_2O_2{\cdot}H_2O$	24.01	0.52
	23.81	0.22

[a] Bold values represent OH stretches. [b] Intensity of complex (I) over that of the isolated subunit (I_0).

were observed. Deviation from the CH stretching frequency model arises in the instances of complexes C and D. In both cases, the frequencies describing the vibrations of the CH involved in coordination of the water molecule through CHO_w interactions are coupled with additional hydrogens involved in similar interactions with the peroxy group of each complex.

CHO Bond Contribution to Stabilization. To help understand the significance CHO bonds make to the stabilization of RO_2 species, the geometry of each complex was scanned in a stepwise optimization in such a way as to isolate the CHO bond as the sole intermolecular interaction. Comparison of the energy of this new structure with that of the original complex shown in Figure 1 can provide an estimate of the portion of the relative binding energy arising from the CHO bond interaction. The results of this scan analysis are given in Table 4. For the complexes surveyed, the CHO bond contributes between 21% ($CH_3O_2{\cdot}H_2O$) and 33% ($CH_3C(O)O_2{\cdot}H_2O$ and $FCH_2CH_2O_2{\cdot}H_2O$). In general, complexes without additional electronegative groups (A and B) have CHO bonds that account for ~20% of the stabilization energy of the molecule. Addition of a hydroxyl- or fluoro- group tends to increase the significance of the CHO interaction by, presumably making the CH group a better proton donor in CHO bond formation. The structures in which a

TABLE 4: CHO Bond Contribution to Complex Stabilization

	C−H···O, %
$CH_3O_2{\cdot}H_2O$	21%
$CH_3CH_2O_2{\cdot}H_2O$	23%
$CH_3C(O)O_2{\cdot}H_2O$	33%
$CH_3C(O)CH_2O_2{\cdot}H_2O$	36%
$CH_2(OH)O_2{\cdot}H_2O$	25%
$FCH_2O_2{\cdot}H_2O$	29%
$FCH_2CH_2O_2{\cdot}H_2O$	33%

carbonyl group is present, and which share a different form of stabilization than do those complexes that do not, have CHO bonds that account for ~35% of the stabilization energy. These results give further evidence to the significance and presence of CHO bond interactions in the stabilization of $RO_2 \cdot H_2O$ complexes.

IV. Discussion

The stability of molecular complexes is a function of the population of gas-phase molecules with sufficient kinetic energy to overcome the binding energies of such complexes through gas-phase collisions. At atmospheric temperatures (200−300 K), a first approximation of the average kinetic energy of molecules and molecular complexes ($3/2k_BT$) can range between 0.60 and 0.89 kcal mol^{-1}. All of the molecular peroxy/water complexes herein investigated have binding energies that are greater than this average by at least 2.5 kcal mol^{-1}. In addition to average kinetic energy considerations, if one assumes that all collisions between two collisional partners take place as they approach each other at an angle of 180° and that all of the kinetic energy involved is transferred to the breaking of the molecular complex, the minimum kinetic energy required by a molecule to break up a molecular complex will be one-half of the binding energy of that complex. Since the kinetic energy distribution of molecules is described by a Boltzmann distribution, the population of gas-phase molecules with sufficient energy for complex dissociation can be approximated by integrating this distribution over the appropriate limits (minimum energy required to infinity). In the case of the weakest peroxy−water complex considered ($CH_3O_2 \cdot H_2O$), ~3.6% of the kinetic energy distribution at 200 K has the required energy for complex dissociation. This percentage increases to ~12.7% at 300 K. For the strongest complex studied [$CH_2(OH)O_2 \cdot H_2O$], these percentages at 200 and 300 K become ~0.05% and 0.77%, respectively. The binding energies reported for each of the peroxy-water complexes suggest that, at tropospheric temperatures, these radical complexes can exist and may play an important role in modifying the peroxy reaction kinetics in much the same way as the HO_2 self-reaction is enhanced in the presence of water.

To further place this consideration into perspective, the lifetimes for the four most prevalent peroxy radical complexes have been calculated as a function of temperature and according to the following relationship:

$$\tau(T) = \frac{1}{\beta_c k^{sc}_{diss,0}[M_T]} \quad (1)$$

where β_c is the collisional efficiency (taken to be unity), $[M_T]$ is the number density of nitrogen molecules at a temperature T, and $k^{sc}_{diss,0}$ is the dissociation constant, as described by Patrick and Golden,[66] using theoretical considerations advanced by Troe.[67] The dissociation constant, $k^{sc}_{diss,0}$, is calculated using eq 2.

$$k^{sc}_{diss,0} = Z_{LJ}\frac{\rho(E_0)RT}{Q_{VIB}}\exp\left(\frac{-E_0}{RT}\right)F_E F_{ANH} F_{ROT} F_{CORR} \quad (2)$$

where Z_{LJ} is the Lennard-Jones collisional frequency (cm^3/molecule s), $\rho(E_0)$ is the density of states calculated using the Whitten-Rabinovitch assumptions,[68,69] R is the gas constant, T is temperature, Q_{VIB} is the vibrational partition function, E_0 is the critical energy, and F_E, F_{ANH}, and F_{ROT} are correction terms for the energy dependence of the density of states, anharmonicity, and rotation, respectively. F_{CORR} is not calculable and is a correction for the coupling that exists between the different types of degrees of freedom as described by Troe[67] and is usually set equal to unity.

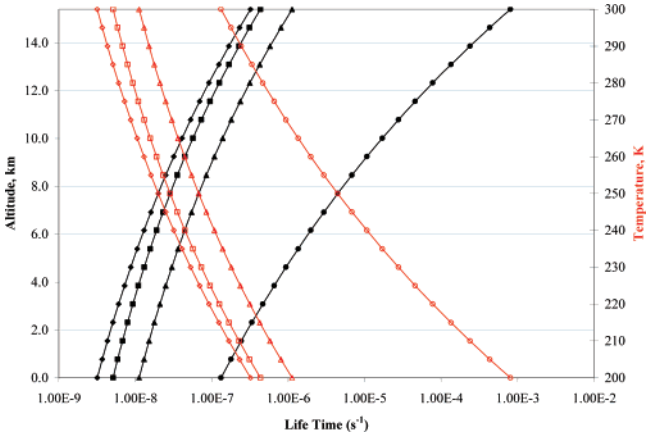

Figure 3. Temperature and altitude versus calculated atmospheric lifetime for the RO_2-H_2O complexes. Temperature profile as a function of altitude is calculated assuming a standard atmospheric profile as described by Arguado and Burt.[72] The black data represent the "altitude vs lifetime" data and the red data represent the "temperature vs lifetime" data. ◆ = $CH_3O_2 \cdot H_2O$; ▲ = $CH_3CH_2O_2 \cdot H_2O$; ■ = $CH_3C(O)O_2 \cdot H_2O$; ● = $HO_2 \cdot H_2O$.

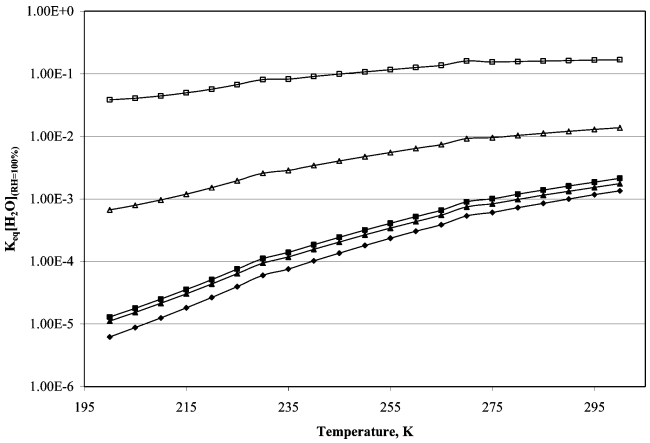

Figure 4. log[K_{eq}*[H_2O]] ([H_2O] at a relative humidity of 100%) as a function of temperature. ◆ = $CH_3O_2 \cdot H_2O$; ▲ = $CH_2CH_2O_2 \cdot H_2O$; ■ = $CH_3C(O)O_2 \cdot H_2O$; □ = $CH_2(OH)O_2 \cdot H_2O$; Δ = $CH_2(OH)CH_2O_2 \cdot H_2O$.

Figure 3 shows the ab initio derived lifetimes of hydroperoxy, methyl peroxy, ethyl peroxy, and acetyl peroxy radical complexes as a function of temperature and altitude, respectively. It also includes that of the hydroperoxy radical complex for perspective. Lifetime calculations for the remaining complexes could not easily be performed as critical thermodynamic quantities are unavailable from the literature. Analysis of Figure 3 shows that as the temperature decreases, the lifetime of the peroxy radical/water complexes increases. This is expected, owing to the decrease in the average kinetic energy of the molecules (assumed to be N_2) colliding with the complex. It is tempting and desirable to demonstrate that a direct relationship exists between the lifetime of each peroxy radical/water complex and its associated binding energy, lifetimes get longer as binding energies increase. This appears to be the case when there is a large difference in binding energies (>1 kcal mol^{-1}), as can be seen by comparing the lifetimes and binding energies of the three $RO_2 \cdot H_2O$ complexes with those of the HO_2-H_2O complex. When binding energies differ by less than 1 kcal mol^{-1}, it appears that the manner of complexation may determine

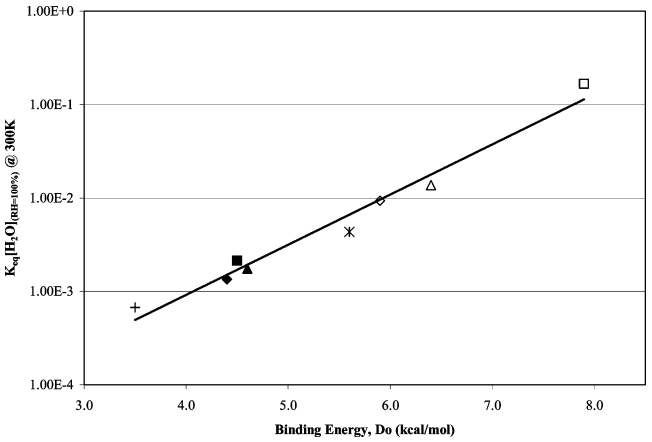

Figure 5. $\log[K_{eq}*[H_2O]]$ ($[H_2O]$ at a relative humidity of 100%) versus zero point corrected binding energy (D_0) (D_0 calculated at the MP2/6-311++G(2df,2p) level) at 300 K. ◆ = $CH_3O_2{\cdot}H_2O$; ▲ = $CH_2CH_2O_2{\cdot}H_2O$; ■ = $CH_3C(O)O_2{\cdot}H_2O$; ◇ = $CH_3C(O)CH_2O_2{\cdot}H_2O$; □ = $CH_2(OH)O_2{\cdot}H_2O$; Δ = $CH_2(OH)CH_2O_2{\cdot}H_2O$; + = $CH_2(F)O_2{\cdot}H_2O$; ∗ = $CH_2(F)CH_2O_2{\cdot}H_2O$.

complex lifetime. The methyl and ethyl peroxy radical/water complex both follow the general trend of forming a complex through hydrogen bond interactions that involve the peroxy functionality itself, and their lifetimes are seen to increase with increasing binding energy. In contrast, the acetyl peroxy complex does not share the common mechanism of complex formation, and its lifetime is shorter than that of the ethyl peroxy complex even though it has a larger binding energy. Each of the calculated lifetimes suggests that these radical-water complexes may have lifetimes of sufficient magnitude as to allow them to perturb their kinetics.

Equilibrium constants were calculated for each of the $RO_2{\cdot}H_2O$ complexes in accordance to theoretical formulations found in McQuarrie et al.[70] and in Steinfeld et al.[71] (see eq 3)

$$K_{eq} = \frac{\left(\frac{q(V,T)}{V}\right)_{complex}}{\left(\frac{q(V,T)}{V}\right)_{water}\left(\frac{q(V,T)}{V}\right)_{RO_2}} \quad (3)$$

where $q(V,T)/V$ is the product of the translational, rotational, vibrational, and electronic partition functions for water, the RO_2 moiety, and the $RO_2{\cdot}H_2O$ complex, as shown in eq 4

$$\frac{q(V,T)}{V} = \left(\frac{2\pi M k_B T}{h^2}\right)^{3/2} \frac{\pi^{1/2}}{\sigma}\left(\frac{T^3}{\Theta_{rot,A}\Theta_{rot,B}\Theta_{rot,c}}\right)^{1/2} \left[\prod_{3n-6}^{j=1} \frac{1}{(1-e^{-\Theta_{vib,j}/T})}\right] g_{e1} e^{-D_e/k_B T} \quad (4)$$

For the group of radical/water complexes under consideration, the magnitude of the equilibrium constant increases with increased binding energy and decreasing temperature. For $CH_3O_2{\cdot}H_2O$ and $HOCH_2O_2{\cdot}H_2O$ at 300 K, K_{eq} was calculated to be 1.54×10^{-21} and 1.91×10^{-19} cm^3 $molecule^{-1}$, respectively. At 200 K, these values increase to 1.02×10^{-19} cm^3 $molecule^{-1}$ for $CH_3O_2{\cdot}H_2O$ and to 6.25×10^{-16} cm^3 $molecule^{-1}$ for $HOCH_2O_2{\cdot}H_2O$.

Useful information regarding the atmospheric abundance of these peroxy radical/water complexes at different relative humidities can be obtained in terms of a ratio between complexed and uncomplexed peroxy radicals by multiplying the equilibrium constant by the relevant $[H_2O]$ concentration, as shown in eq 5

$$K_{eq}[H_2O] = \frac{[RO_2{\cdot}H_2O]}{[RO_2]} \quad (5)$$

Figure 4 plots this ratio as a function of temperature at 100% humidity. As expected, the relative abundance of the complex increases relative to the uncomplexed peroxy radical as the abundance of atmospheric moisture increases with temperature. When the logarithm of this ratio is plotted against the complex binding energies, a linear relationship is obtained. Figure 5 is such a plot for the eight $RO_2{\cdot}H_2O$ complexes reviewed, as well as $HO_2{\cdot}H_2O$. A plot such as this is a powerful indicator of expected ratios ([complex]/[RO_2])of atmospherically present peroxy radicals as a function of binding energy. Many atmospheric modeling studies have ignored the water influence on RO_2 abundances and RO_2 chemistry; our findings suggest that water will play an important role in influencing the abundances of RO_2.

V. Conclusions

The existence of $RO_2{\cdot}H_2O$ complexes is postulated to play a part in the initial formation of aerosols. In order for peroxy water complexes to have significant participation as aerosol initiators through the proposed reverse micelle mechanism, they must have binding energies that are larger than $3/2k_BT$. Examination of the $RO_2{\cdot}H_2O$ series considered in this manuscript indicates that any member of the series may contribute, but we predict those with the largest binding energies (>5 kcal mol^{-1}) are most likely to play a significant contributing role because of their longer atmospheric lifetimes. Based on this trend, these results suggest that the kinetics of organic peroxy radical water complexes will be perturbed in relation to the magnitude of their respective binding energies. Moreover, hydroxyl containing organic peroxy radicals would more likely modify the kinetics and the resulting product branching ratio for peroxy self-reactions, peroxy-cross reactions, and reactions with NO_x. As such, the product branching ratios of RO_2 + NO reactions in the presence of water will deviate from those run in the absence of water, much like the recent results published by Butkovskaya[7] et al.

This work illustrates the potential importance of organic peroxy radical-water complexes by their range of binding energy and atmospheric lifetime for a series of organic peroxy radicals. The spread in binding energies can be explained by the composition of the R group attached to the peroxy moiety. The general trend in binding energies has been determined to be: fluorine ≈ alkyl < carbonyl < alcohol. The weakest bound complex, $FCH_2O_2{\cdot}H_2O$, is calculated to be bound by 2.1 kcal mol^{-1} and the strongest, $[CH_2(OH)O_2{\cdot}H_2O]$, is bound by 5.1 kcal mol^{-1}. The modest binding energy of the peroxy radical-water complexes which contain carbonyl and alcohol groups indicates that these complexes may play important chemical roles under low-temperature conditions, as for example in atmospheric or interstellar chemical processes.

Acknowledgment. The authors express their gratitude to Dr. Tapas Kar for his experience in generating the electron density difference maps and Dr. Steve Scheiner and Dr. Randy Shirts for very helpful discussions leading to the publication of this manuscript. Recognition is made to the National Science Foundation (Grant No. 0631167) for support of the present work.

References and Notes

(1) Lightfoot, P. D.; Cox, R. A.; Crowley, J. N.; Destriau, M.; Hayman, G. D.; Jenkin, M. E.; Moortgat, G. K.; Zabel, F. *Atmos. Environ.* **1992**, *26A*, 1805.

(2) Wallington, T. J.; Dagaut, P.; Kurylo, M. J. *Chem. Rev.* **1992**, *92*, 667.

(3) Blanksby, S. J.; Ramond, T. M.; Davico, G. E.; Nimlos, M. R.; Kato, S.; Bierbaum, V. M.; Lineberger, W. C.; Ellison, G. B.; Okumura, M. *J. Am. Chem. Soc.* **2001**, *123*, 9585.

(4) Kircher, C. C.; Sander, S. P. *J. Phys. Chem.* **1984**, *88*, 2082.

(5) Darnall, K. R.; Carter, W. P. L.; Winer, A. M.; Lloyd, A. C.; Pitts, J. N. *J. Phys. Chem.* **1976**, *80*, 1948.

(6) Atkinson, R. *J. Phys. Chem. Ref. Data* **1997**, *26*, 215.

(7) Butkovskaya, N. I.; Kukui, A.; Pouvesle, N.; Le, Bras, G. *J. Phys. Chem. A* **2005**, *109*, 6509.

(8) Suma, K.; Sumiyoshi, Y.; Endo, Y. *Science* **2006**, *311*, 1278.

(9) Kanno, N.; Tonokura, K.; Tezaki, A.; Koshi, M. *J. Phys. Chem. A* **2005**, *109*, 3153.

(10) Aloisio, S.; Francisco, J. S. *J. Phys. Chem. A* **1998**, *102*, 1899.

(11) Stockewell, J. *J. Geophys. Res.* **1995**, *110*, 11695.

(12) Donaldson, D. J.; Vaida, V. *Chem. Rev.* **2006**, *106*, 1445.

(13) Ellison, G. B.; Tuck, A. F.; Vaida, V. *J. Geophys. Res.* **1999**, *104*, 11633.

(14) Dobson, C. M.; Ellison, G. B.; Tuck, A. F.; Vaida, V. *Proc. Natl. Acad. Sci.* **2000**, *97*, 11864.

(15) Vaida, V.; Tuck, A. F.; Ellison, G. B. *Phys. Chem. Earth* **2000**, *25*, 195.

(16) Frisch, M. J.; Trucks, G. W.; Schlegel, H. B.; Scuseria, G. E.; Robb, M. A.; Cheeseman, J. R.; Zakrzewski, V. G.; Montgomery, J. A.; Stratmann, R. E.; Burant, J. C.; Dapprich, S.; Millam, J. M.; Daniels, A. D.; Kudin, K. N.; Strain, M. C.; Farkas, O.; Tomasi, J.; Barone, V.; Cossi, M.; Cammi, R.; Mennucci, B.; Pomelli, C.; Adamo, C.; Clifford, S.; Ochterski, J.; Petersson, G. A.; Ayala, P. Y.; Cui, Q.; Morokuma, K.; Rega, N.; Salvador, P.; Dannerberg, J. J.; Malick, D. K.; Rabuck, A. D.; Raghavachri, K.; Foresman, J. B.; J, C.; Oritz, J. V.; Baboul, A. G.; Stefanov, B. B.; Liu, G.; Liashenko, A.; Piskorz, P.; Komaromi, R.; Gomperts, R.; Martin, R. L.; Fox, D. J.; Keith, T.; Al-Laham, M. A.; Peng, C. Y.; Nanayakkara, A.; Challacombe, P. M.; Gill, P. M. W.; Johnson, B.; Chen, W.; Wong, M. W.; Andres, J. L.; Gonzalez, C.; Head-Gordon, M.; Repogle, E. S.; Pople, J. A. Gaussian 98, revision A.11.3; Gaussian, Inc: Pittsburgh, PA, 2002.

(17) Moller, C.; Plesset, M. S. *Phys. Rev* **1934**, *46*.

(18) Pople, J. A.; Head-Gordon, M.; Raghavachri, K. *J. Chem. Phys.* **1987**, *87*.

(19) Pople, J. A.; Head-Gordon, M.; Raghavachri, K. *J. Chem. Phys.* **1989**, *90*.

(20) Purvis, G. D. I.; Bartlett, R. J. *J. Chem. Phys.* **1982**, *76*.

(21) Lee, T. J. *J. Chem. Phys.* **1991**, *69*.

(22) Handy, N. C.; Pople, J. A.; Head-Gordon, M.; Raghavachri, K.; Trucks, G. W. *Chem. Phys. Lett.* **1989**, *164*.

(23) Scuseria, G. E. *Chem. Phys. Lett.* **1994**, *226*.

(24) Slater, J. C. *Phys. Rev.* **1930**, *35*, 210.

(25) Fock, V. *Z. Physik* **1930**, 126.

(26) Hartree, D. R.; Hartree, W. *Proc. R. Soc.* **1935**, 9.

(27) Stephens, P. J.; Devlin, F. J.; Chabalowski, C. F.; Frisch, M. J. *J. Phys. Chem.* **1994**, *98*, 11623.

(28) Becke, A. D. *J. Chem. Phys.* **1993**, *98*, 5648.

(29) Lee, C.; Yang, W.; Parr, R. G. *Phys. Rev. B* **1988**, *37*, 785.

(30) Vosko, S. H.; Wilk, L.; Nusair, M. *Can. J. Phys.* **1980**, *58*, 1200.

(31) Hariharan, P. C.; Pople, J. A. *Theor. Chim. Acta* **1973**, *28*, 213.

(32) Krishnan, R.; Binkley, J. S.; Seeger, R.; Pople, J. A. *J. Chem. Phys.* **1980**, *72*, 650.

(33) Clark, T.; Chandrasekhar, J.; Spitznagel, G. W.; Schleyer, P. v. R. *J. Comput. Chem.* **1983**, *4*, 294.

(34) Ditchfield, R.; Hehre, W. J.; Pople, J. A. *J. Chem. Phys.* **1971**, *54*.

(35) Frisch, M. J.; Pople, J. A.; Binkley, J. S. *J. Chem. Phys.* **1984**, *80*.

(36) Planck, M. *Verhandlungen der Deutschen Physikalischen Gesellschaft* **1911**, *13*.

(37) Einstein, A.; Stern, O. *Ann. Phys.* **1913**, *40*.

(38) Boys, S. F.; Bernardi, F. *Mol. Phys.* **1970**, *19*, 553.

(39) Jensen, F. *Introduction to Computational Chemistry*, 2 ed.; Wiley: New York, 2006.

(40) Latajka, Z.; Scheiner, S. J. *J. Chem. Phys.* **1987**, *87*, 1194.

(41) Reed, A. E.; Curtiss, L. A.; Weinhold, F. *Chem. Rev.* **1988**, *88*, 899.

(42) Clark, J. Hansen Lab Software Provo, 2006.

(43) Gu, Y.; Kar, T.; Scheiner, S. *J. Am. Chem. Soc.* **1999**, *121*, 9411.

(44) Popelier, P. L. A.; Koch, U. *J. Phys. Chem.* **1995**, *99*, 9747.

(45) Egli, M.; Gessner, R. V. *Proc. Natl. Acad. Sci.* **1995**, *92*, 180.

(46) Berger, I.; Egli, M.; Rich, A. *Proc. Natl. Acad. Sci.* **1996**, *93*, 12116.

(47) Ornstein, R. L.; Zheng, Y. J. *J. Biomol. Struct. Dyn.* **1997**, *14*, 657.

(48) Takahara, P. M.; Frederick, C. A.; Lippard, S. J. *J. Am. Chem. Soc.* **1996**, *118*, 12309.

(49) Jiang, L.; Lai, L. *J. Biol. Chem.* **2002**, *277*, 37732.

(50) Derewenda, Z. S.; Lee, L.; Derewenda, U. *J. Mol. Biol.* **1995**, *252*, 248.

(51) Bella, J.; Berman, H. M. *J. Mol. Biol.* **1996**, *264*, 734.

(52) Musah, R. A.; Jensen, G. M.; Rosenfeld, R. J.; McRee, D. E.; Goodin, D. B.; Bunte, S. W. *J. Am. Chem. Soc.* **1997**, *119*, 9083.

(53) Steiner, T.; Saenger, W. *J. Am. Chem. Soc.* **1992**, *114*, 10146.

(54) Steiner, T.; Saenger, W. *J. Am. Chem. Soc.* **1993**, *115*, 4540.

(55) Allen, F. H.; Bellard, S.; Brice, M. D.; Cartwright, B. A.; Doubleday, A.; Higgs, H.; Hummelink, T.; Hummelink-Peters, B. G.; Kennard, O.; Motherwell, W. D. S.; Rodgers, J. R.; Watson, D. G. *Acta Crystallogr., Sect. B* **1979**, *B35*, 2331.

(56) Christensen, L. E.; Okumura, M.; Hansen, J. C.; Sander, S. P.; Francisco, J. S. *J. Phys. Chem. A* **2006**, *110*, 6948.

(57) Aloisio, S.; Francisco, J. S.; Friedl, R. R. *J. Phys. Chem. A* **2000**, *104*, 6597.

(58) Steiner, T. *Chem. Commun.* **1997**, 727.

(59) van de Bovenkamp, J.; Matxain, J. M.; van Duijneveldt, F. B.; Steiner, T. *J. Phys. Chem A* **1999**, *103*.

(60) Steiner, T.; Kanters, J. A.; Kroon, J. *Chem. Commun.* **1996**.

(61) Brandl, M.; Lindaur, K.; Meyer, M.; Suhnel, J. *Theor. Chim. Acta* **1999**, *101*.

(62) Mizuno, K.; Ochi, T.; Shindo, Y. *J. Chem. Phys.* **1998**, *109*.

(63) Hobza, P.; Spirko, V.; Havlas, Z.; Buchhold, K.; Reimann, B.; Barth, H.-D.; Brutschy, B. *Chem. Phys. Lett.* **1999**, *299*.

(64) Chaney, J. D.; Goss, C. R.; Folting, K.; Santarsiero, B. D.; Hollingsworth, M. D. *J. Am. Chem. Soc.* **1996**, *118*.

(65) Bedell, B. L.; Goldfarb, L.; Mysak, E. R.; Samet, C.; Maynary, A. *J. Phys. Chem. A* **1999**, *103*.

(66) Patrick, R.; Golden, D. M. *Int. J. Chem. Kinet.* **1983**, *15*, 1189.

(67) Troe, J. *J. Chem. Phys.* **1977**, *66*, 4745.

(68) Tardy, D. C.; Rabinovitch, B. S.; Whitten, G. Z. *J. Chem. Phys.* **1968**, *48*, 1427.

(69) Whitten, G. Z.; Rabinovitch, B. S. *J. Chem. Phys.* **1963**, *38*, 2466.

(70) McQuarrie, D. A.; Simon, J. D. *Physical Chemistry: A Molecular Approach*, 1st ed.; University Science Books, 1997.

(71) Steinfeld, J. I.; Francisco, J. S.; Hase, W. L. *Chemical Kinetics and Dynamics*; Prentice Hall: New York, 1989.

(72) Rohli, R. V.; Schmidlin, T. W.; Aguado, E.; Burt, J. E. *Understanding Weather and Climate*; Prentice Hall: New Jersey, 1999.